Multicellular dosimetry for beta-emitting radionuclides: Autoradiography, thermoluminescent dosimetry and three-dimensional dose calculations

E. D. Yorke
George Washington University Medical Center, Washington, DC 20037

L. E. Williams and A. J. Demidecki
City of Hope Medical Center, Duarte, California 91010

D. B. Heidorn and P. L. Roberson
University of Michigan Medical School, Ann Arbor, Michigan 48109

B. W. Wessels
George Washington University Medical Center, Washington, DC 20037

(Received 18 March 1992; accepted for publication 23 November 1992)

Inhomogeneities in activity distributions over distances from 10 to 10^4 μm are observed in many tumors treated with radiolabeled antibodies. Resulting nonuniformities in absorbed dose may have consequences for the efficacy of radioimmunotherapy. Activity variations may be directly studied with quantitative autoradiography (ARG). Converting these data to absorbed dose distributions requires additional information about pharmacokinetics, the use of a point source function and consideration of the complete three-dimensional activity distribution, as obtained from sequential autoradiographic slices. Thermoluminescent dosimetry with specially prepared $CaSO_4$:Dy dosimeters implanted into tissue can directly measure absorbed dose in selected regions. The conditions under which thermoluminescent dosimeters (TLD) are used differ markedly from "normal" use conditions in external beam radiotherapy. Therefore special calibration and quality assurance precautions are needed to assure the precision of this technique. Procedures and pitfalls in the use of both techniques in radioimmunotherapy are described.

I. INTRODUCTION

A major concern of external beam radiotherapy is the design of beam configurations which produce a uniform dose distribution over the tumor volume. In radioimmunotherapy, (RIT) as with other radiopharmaceutical therapies, the activity distribution is determined by biological factors with large associated uncertainty. Nonuniform distributions of activity and of absorbed dose may result.

The technique of autoradiography (ARG) is well known.[1] For over a decade ARG has been used to demonstrate activity heterogeneity on the multicellular size scale (10–10^4 μm) for conventional radiopharmaceuticals[2–4] and more recently for radiolabeled antibodies.[5–7] The film density may be calibrated with standard activity samples, leading to quantitative measurements of activity of distributions with submillimeter spatial resolution in the plane of the tissue section.

Calculations of absorbed dose distributions for idealized activity distributions of beta particle emitters demonstrate that when the absorbed dose is delivered primarily by particulate radiation of short range, heterogeneous activity distributions will lead to doses which are nonuniform on approximately the same distance scale.[8–11] Autoradiography frequently reveals irregular activity distributions in tumors. In such situations, calculations based upon geometrically simple shapes are of limited utility. Quantitative ARG can provide the spatial activity distribution needed to calculate instantaneous dose rate distributions. But this technique cannot yield total absorbed dose distributions without further assumptions. This is because absorbed dose distributions are as much determined by pharmacokinetics of antibody uptake and clearance as by the geometric distribution of activity. Autoradiography, however, shows only a "freeze frame" of the activity distribution at the time the tumor was resected and frozen.

Direct *in vivo* measurements of cumulative doses to tissues during RIT can be made using thermoluminescent dosimeter(s) (TLD). This technique is well established in medical and health physics.[12,13] TLD materials used for RIT beta dosimetry must meet some special criteria. The physical size of the dosimeter should be small compared to the average beta range (e.g., 0.4 mm for I-131) in order that the dosimeter not perturb the dose distribution in its vicinity. Small size is also necessary to assure good spatial resolution and to avoid disruption of the tissues into which they are implanted. The light output per unit absorbed dose must be large enough to produce a useful signal despite the small volume of material. Additionally, since the absorbed dose is delivered by a spectrum of beta particles, it is necessary to choose a material whose thermoluminescent response is insensitive to beta energy for the radionuclide of interest. Using TLD that meet these criteria, large variations in absorbed dose in association with autoradiographs which show strong activity heterogeneity have been directly measured.[7]

ARG and thermoluminescent dosimetry are complementary techniques. ARG provides a wealth of "geo-

 0094-2405/93/020543-08$01.20

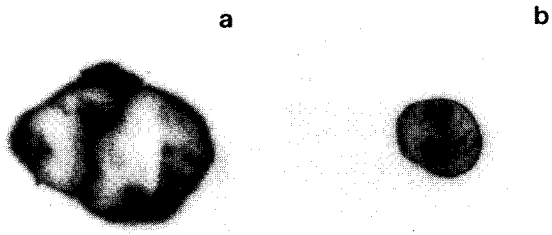

FIG. 1. Section autoradiographs from subcutaneous xenografts in athymic nude mice taken one day post injection with I-131 labeled monoclonal antibody. (a) LS174T human colon cancer with 300 μCi 17-1A monoclonal antibody; (b) Raji human Burkitt lymphoma xenograft with 100 μCi anti-B-1 pan-B-cell monoclonal antibody.

graphic" data relating to the activity distribution at a single instant of time. To proceed from a set of autoradiographs to a dose distribution requires a pharmacokinetic model as well as an algorithm for adding the contributions to the dose at a chosen point from all the activity within range of that point. More than one tissue slice must be considered even if the dose distribution in only one slice is desired. The TLD crystal is an integrating dosimeter. It performs the necessary spatial and temporal integrations, but only within the very limited volume that it occupies. Methods and questions relating to both these techniques, as well as possible fruitful ways to combine them are discussed in the following sections.

II. AUTORADIOGRAPHY

Autoradiography (ARG) is a unique method for the graphical display of activity heterogeneity on the multicellular size scale of particular interest in RIT with medium to high energy beta particles. Although detectors other than film are being investigated,[14,15] the discussion below is limited to film ARG.

Typically, the tissue sample of interest is frozen in liquid nitrogen and divided into sections of known thickness with a microtome. The frozen sections are mounted, air dried and then either placed in contact with the emulsion side of the film or separated from it by a thin cover or dipped into emulsion so that the specimen is covered with a thin emulsion layer. Exposure times must be chosen to avoid either underexposing or saturating the film and thus will depend on the sample activity, the radionuclide and the film used. Times from 1 h to approximately a week have been used. Example autoradiographs are shown in Fig. 1.

Although homogenous activity distributions are seen in many tissue samples, they are not universally observed. Numerous workers have reported heterogeneous uptake of radiolabeled antibody in tumors.[5–7,16,17] Some patterns of uptake commonly seen include concentration of activity near the periphery of the tumor and near tumor vasculature.

To use ARG to quantitate activity distributions, it is necessary to choose film that will be sensitive to beta particles of medium to high energy. Intensifying screens will degrade resolution and may cause reciprocity failure[1] but may be necessary with some films. They were not used in Refs. 7 and 16 (LKB "Ultrofilm") but were used in Ref. 17 (X-OMAT XTL-2). The exposure time for each autoradiograph should be recorded.

Conversion of optical density to activity requires calibration of the film using gel wafers of known thickness and known uniform activity. The calibration curve depends on radionuclide, section thickness, exposure conditions, film development conditions, and (if reciprocity failure is present) exposure rate. An independent calibration check should be performed for each group of autoradiographs. The calibration gels are left in contact with film for known times under the same exposure conditions as used for the tissue samples. Development conditions should be the same for calibration and autoradiographic films. A calibration curve of optical density as a function of cumulated specific activity of the gel is thus generated. The curve can be used to find the average cumulated specific activity for a small volume of interest of the autoradiographic tissue sample. If the calibration gels and the tissue slices are of different thickness, a correction factor should be applied.[7] The correction factor may be measured using gel samples of different thicknesses. Since the autoradiograph exposure time is known and physical decay of the radionuclide is the only process causing activity changes during autoradiography, the specific activity at the beginning of autoradiography can be determined.

With an optical density scan of the film, a map of the specific activity distribution over a grid of voxels can be generated. The densitometer readout resolution (spot size) should be small to help minimize the change in optical density over the aperture. Because the optical density varies with the logarithm of the light transmittance, the densitometer reading will not reflect the average optical density if there is a large gradient over the spot size diameter.[18] Automated approaches to grain density determination techniques with higher spatial resolution are being explored.[19] The volume of a voxel is determined by the readout grid spacing and the slice thickness. The two-dimensional section images are stacked to yield a three-dimensional activity density matrix and can also be used to form a surface description.

Video digitization or laser densitometry techniques are useful in dealing in a quantitative fashion with the abundant data provided by ARG. For example, with 100-μm resolution of the densitometer and 50-μm-thick adjacent tissue slices, a set of autoradiographs of a $5\times5\times5$ mm tumor provides information on the specific activity in 2.5×10^5 voxels.

The specific activity distribution can be used to calculate a three dimensional absorbed dose rate distribution. An example is shown in Fig. 2. Using the activity per voxel to calculate dose rate distributions is computationally intensive. The dose rate at a point is the sum of contributions from all the voxels lying within the maximum beta range.

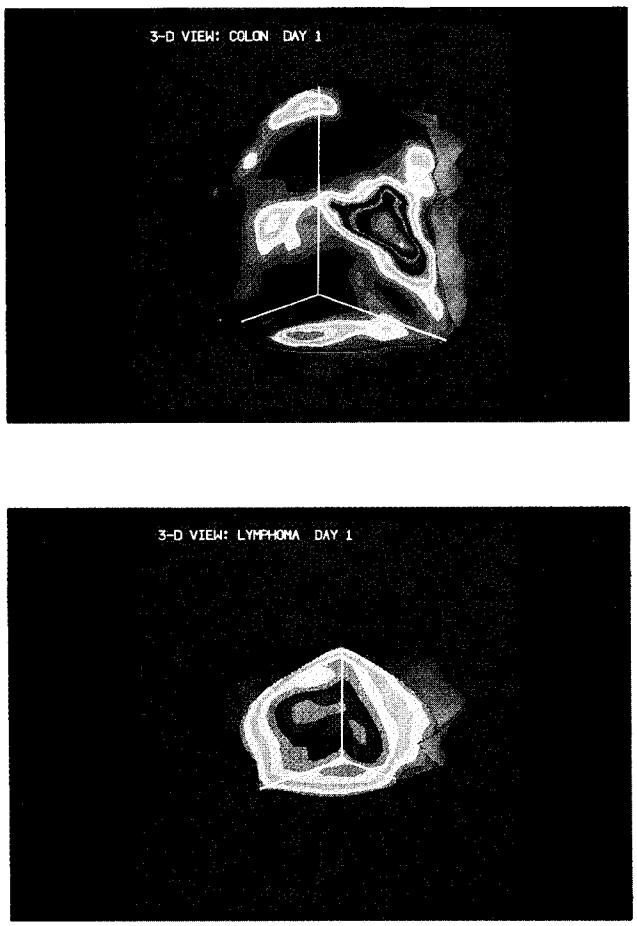

FIG. 2. Three-dimensional dose rate distributions for tumor xenografts from Fig. 1. The color scale is black, dark blue, light blue, pink, light green, dark green, light peach, dark peach, dark red, red, orange in equal ascending dose-rate intervals. Higher dose rate regions cycle back to black, dark blue, etc. (a) LS174T human colon cancer with 17-1A monoclonal antibody, dose-rate interval 2.5 cGy/h, mean dose rate 7.6 cGy/h; (b) Raji human Burkitt lymphoma xenograft with anti-B-1 pan-B-cell monoclonal antibody, dose-rate interval 0.4 cGy/h, mean dose rate 2.4 cGy/h.

This includes voxels both in and out of the autoradiographic slice containing the point of interest. A suitable point source function must be used to provide the distance dependence appropriate to the radionuclide.[20–23] Roberson *et al.*[17] adapted brachytherapy software to perform this task. A "voxel dose rate distribution" per unit activity was generated using up to 500 equally spaced point sources distributed over a voxel and the dose point kernel of Ref. 21. This voxel dose rate calculation was carried out beyond the range of the beta particles. Each of 5000 to 8000 voxel positions (0.5-mm voxel spacing for I-131) were assigned the voxel dose rate distribution, weighted by the specific activity in that voxel. The source distributions were then summed in three dimensions. The calculation time investment (100–200 h on a VAX 8800) limited the number of source positions which could be used. Based on the mean beta range, the optimal voxel size for I-131 is approximately 100 μm, which increases the number of source points by a factor of 125. To reduce the calculation time, Fourier transforms could be used.[9]

In general, activity distributions which vary over distances comparable to the beta particle range will produce dose-rate distributions which vary strongly over the same length scale. Smaller scale (less than beta range) activity heterogeneities will produce less dramatic dose rate variations, since the dose at a point is delivered by beta particles from both "hot" and "cold" portions of the tissue.[7–11,17,24] Thus computational effort to produce three-dimensional dose or dose rate distributions depends on the range of the beta particles and the tumor size.

Conversion of the activity distributions obtained by ARG to the cumulative absorbed dose distribution produced during the administration of RIT—that is, during the time that the tissue was in a living host—is not straightforward. The dose distribution depends on the individualized pharmacokinetics of the radiolabeled antibody *in vivo*. The autoradiograph provides only a "freeze frame" view of the activity distribution at the time of tumor resection. At best ARG gives indirect information about the time dependence of the biological processes of uptake and clearance of the antibody during the RIT.

To provide the necessary missing kinetic information, it might be possible to model the pharmacokinetics. Diffusion model equations have been applied to dosimetry calculations for multicellular spheroids[25] and simulated tumor nodules.[26] It may be possible to extend such models to tumors *in vivo* to provide kinetic input to cumulated dose distribution calculations.

In an alternative approach many groups have measured average specific activity as a function of time for tumors and various organs by noninvasive imaging techniques in humans and by serial sacrifice in small animal models for a variety of antibody carrier/radionuclide combinations.[27–30] Assumptions must then be made as to how small scale heterogeneities vary with time (e.g., do "hot" and "cold" regions remain in the same ratio to the average throughout RIT?). The resulting time dependence must be combined with the radionuclide's physical decay to obtain a model cumulated activity distribution based on the autoradiographic information. While several groups have discussed such a program, it has not yet been carried out. Griffith, *et al.*[7] used purely physical decay to generate dose distributions from autoradiographs. Recently Roberson, *et al.*[17,24] generated three-dimensional dose rate distributions characteristic of discrete times of sacrifice and recommended sampling the dose rate distributions at a minimum of four to six time points.[24] For tumors which were approximately matched in size, the variability in dose per volume element was observed to be small compared to the variability at different time points. Thus it might be possible to sum dose rate calculations from different tumors, resected at different time points, by identifying areas of similar composition (e.g., similar vascularization and/or proximity to the periphery). Further work is needed to develop and validate models of antibody carrier pharmacokinetics on the multicellular size scale in order to reliably translate the activity distributions visualized with

quantitative autoradiography into absorbed dose distributions.

III. THERMOLUMINESCENT DOSIMETRY

Studies done with thermoluminescent dosimetry give information which is complementary to that provided by ARG. TLD materials are crystalline solids in which ionizing radiation can excite electrons into metastable trapped states. The number of such electrons is proportional to the absorbed dose received. The electrons can be released from these states by heating. Thereupon they recombine with holes, giving off excess energy in the form of thermoluminescent photons, which can be counted with a photoelectric tube. The light output is proportional to the absorbed dose received by the TLD but also depends on material properties, irradiation conditions, heating conditions, and the electronics of the TLD reader. Therefore, if thermoluminescent dosimeters are to be used for absorbed dose measurements, they must be calibrated.

Appropriately calibrated TLD implanted directly into tissue yields the total dose absorbed by the TLD material during its time *in situ*. The TLD automatically integrates over the spatial and temporal distribution of all the activity within the beta particle range of its location (and, of course, also accounts for the absorbed dose contributed by penetrating radiation from distant sites). However, the dose in only a small volume is recorded, as opposed to the global *activity* distribution information provided by ARG.

The conditions under which TLD are used in RIT dosimetry differ markedly from those in health physics or radiation therapy. This leads to special requirements in the fabrication and calibration of the dosimeters. As noted in the Introduction, the TLD must be of small cross section compared to the beta particle range. Wessels and coworkers found that $CaSO_4$:Dy met the dual requirements of high sensitivity (light output gm^{-1} cGy^{-1}) and weak energy dependence for I-131 and higher energy beta emitters.[31] They and others[7,27,32–39] have fabricated TLDs of dimensions $0.2\times0.4\times5$ mm or less, implanted them into animals or tumor model systems receiving RIT and performed *in vivo* absorbed dose measurements. Techniques of fabrication, quality assurance, calibration and *in vivo* use of these TLDs were developed by Wessels and Griffith.[7,31] Similar procedures have been adopted at approximately 15 institutions including those involved in Refs. 32–39. In the following discussion, $CaSO_4$:Dy dosimeters are emphasized because of their extensive application in RIT dosimetry.

The starting materials are 400-μm-thick 1.2-cm-diameter $CaSO_4$:Dy impregnated teflon disks (Teledyne, Inc.). The disks are imbedded in a 2×2 cm paraffin block and sliced with a well-sharpened tissue section microtome to a thickness of 200 μm and a length of 500 μm, yielding dosimeters of final dimensions $0.2\times0.4\times5$ mm. These dosimeters conveniently fit inside a 20-gauge needle. Each dosimeter is measured (by micrometer) to insure geometric batch uniformity ($\pm3\%$). For initial studies[31] the dosimeters were also weighed using a microgram balance.

After being cut, the excess paraffin is removed and the TLD are annealed. External beam calibration may be performed using a calibrated low megavoltage (4 MV or Co-60) beam with full buildup. The dosimeters are then read in a commercial TLD reader under dry nitrogen. Different groups have used slightly different heat cycle settings (e.g., Ref. 7 uses a 5-s preheat at 115° followed by glow peak integration over 50 s from 115 °C to 275 °C with temperature ramping at 3.6 °C/s). Batches of "mini-TLD" with response uniformity better than $\pm10\%$ are readily obtained.

Linearity of light output (LO) versus dose should be measured with external beam over the entire range of absorbed doses expected in RIT (5 to 5000 cGy). Deviation of a log–log plot of LO versus absorbed dose from a 45° line indicates supralinearity or saturation. Supralinearity has been reported above 500 cGy by some workers[36,40] but not seen up to 1000 cGy by others.[29] This effect may depend on the batch of material or on preparation techniques. Supralinearity can be appreciable. Demidecki and co-workers have seen an increase by a factor of 1.7 of the LO per cGy or calibration factor as absorbed dose is increased from 50 to 3000 cGy.[40,41] Therefore it is essential to use a measured dose-response curve and not to assume that the calibration factor is independent of dose.

External beam exposures are of short (minutes) duration, after which the TLD material is stored in air at room temperature and usually read out within 1–2 days. In RIT applications, the TLD is imbedded in tissue at mammalian body temperature and physiological *p*H. The tissue contains an activity distribution of beta-emitting radionuclide, exposing the TLD to low dose rate (approximately 10 cGy/hr) beta and gamma radiation for times ranging from a few days to two weeks. Upon removal, the TLD must be cleaned of residual tissue before being read. The TLD is a relative dosimeter; absorbed dose in an investigational situation is determined by the ratio of the LO to the output from a similar (or the same) TLD given a known dose. Additional calibration should therefore be performed under conditions which closely resemble the conditions of actual use, as the calibration factor may well depend on these conditions.

For this purpose the TLD are cross calibrated with uniform activity distributions of the radionuclide of interest. The dosimeters are immersed for times ranging from minutes to 2 weeks in gels (e.g., Knox Gelatin) prepared with known uniform activity. After removal from the gel, each dosimeter must be thoroughly washed and then read on the TLD reader. The calibration medium is large compared to the beta range so the absorbed dose to the medium can be calculated via the beta particle equilibrium dose constant and an absorbed fraction of one. If the TLD are to be used under conditions where the penetrating radiation dose is expected to be important, calibration in a larger phantom or with an added external x-ray irradiation might be advisable to obtain a combined calibration factor.

The radionuclide calibration factor may well be different from the standard external x-ray beam factor. Reference 31 reports the same ($\pm5\%$) factor for 4 MV as for

I-131, Y-90 and P-32 gels. However, in later work from the same laboratory, I-131 calibration factors as low as 60% of the 4-MV factor were measured and a calibration factor of approximately 70% was measured for a smaller ($0.1 \times 0.14 \times 2.5$ mm) set of TLD.[39] Heidorn observed a similar (approximately 40%) discrepancy between Co-60 and I-131.[42] Stewart *et al.*[43] saw similar differences between 4-Mev electrons and I-131 solutions using $6 \times 1 \times 1$ mm Lif rods while Y-90 solution data coincided with 4-Mev electrons.

There are at least three reasons for expecting a difference in calibration factor between external megavoltage x-rays and beta particle irradiation in solution or gel.

(1) The LO of the TLD may have intrinsic energy dependence. This may be checked using external irradiation at different nominal electron beam energies or with beta sources. At least part of this effect is due to the thickness of the TLD relative to the beta particle range in TLD material.[44] Demidecki, *et al.* find that for Y-90, the energy dependence is within 10% for mini-TLD.[41]

(2) In radioactive gel or solution, the finite size of the TLD excludes radioactive material from points within its volume. Demidecki, *et al.* have called this the "void volume" effect.[20,41] The absence of radioactivity reduces the absorbed dose to the TLD. Demidecki *et al.* have performed calculations of this effect for Y-90 and I-131. The dose reduction depends on the TLD density as well as its size (i.e., on the beta particle range versus TLD size). Calculations[41] indicate that especially for I-131, the predicted decrease in calibration factor relative to 4-MV x-rays is substantial.

(3) The LO of the TLD also varies with time in the medium. When the TLD are irradiated with external beam and stored in air at room temperature, they show less than 5% fading per month. However, for irradiation in medium over days to weeks, the fading properties depend upon the medium (e.g., temperature and *p*H) as well as the time in the medium and the total dose. The surface to volume ratio of the TLD material probably plays a role; the effect may also depend on the batch of material purchased from the vendor.

Experiments performed by Wessels and co-workers from 1984 to 1988 with one group of TLD material showed no fading for TLD irradiated in aqueous media[31] at room temperature. However, experiments with newer material by Demidecki and collaborators,[41] and Svenberg[45] show fading by a factor of up to 50% in 20 days for mini-TLD irradiated in Y-90 gel for 20 days. The effect is larger for geometries with a larger surface to volume ratio. For a 6-mm diameter, 20-μm-thick $CaSO_4$:Dy disk, Demidecki *et al.*[40,41] report an approximately exponential decrease in LO with time by a factor of five over 20 days in cell medium and by a factor of 10 for the same time in gel. This fading appears to be irreversible. After the TLD has been cleaned, read, and annealed it does not regain its initial sensitivity.

Since it is not presently possible to theoretically account for these effects, it is necessary to calibrate the dosimeters for *in vivo* RIT dosimetry using conditions as close as possible to those under which they are used. This will minimize the impact of *p*H, temperature and the "void volume" effect and will help account for possible interplay between supralinearity and fading.

The mini-TLD can be implanted into animal models undergoing RIT and left in place for days to several weeks. They can also be implanted into animals receiving external beam (e.g., 4 MV) irradiation to a known dose as a check on the effect of biological conditions on the thermoluminescent response. A recent study reports fading under these circumstances.[46] Mini-TLD have also been extensively checked for signs of degradation due to biological conditions.[7] None were seen. Before reading a TLD which has been implanted in tissue it is important that it be carefully cleaned and dried.

In RIT, the mini-TLD yield an average (over the length of the dosimeter) dose to the nearby surrounding tissue. Agreement with average doses calculated from organ or tumor-average cumulated activities obtained by serial sacrifice of similarly treated animal models is generally good.[27,33,34] These calculations have incorporated boundary corrections as necessary for organs or tumors which are small compared to the beta particle range. Activity heterogeneity within the tissue is not included. In this work, possible fading due to time in aqueous medium, *p*H, temperature and "void volume" effects have been corrected for, at least in part, by appropriate calibration.

The mini-TLD have good spatial resolution for dose gradients along their thin (0.2 and 0.4 mm) dimensions. However the LO depends on the summed dose along the long (5 mm) axis. Steep dose gradients were measured in cylindrical phantoms containing I-131, Y-90, and P-32.[31] The spatial resolution along the 5-mm axis can be extracted by slicing the dosimeter. This is the technique which was applied in conjunction with autoradiography.[7] The tissue sample containing the TLD was quickly frozen in liquid nitrogen. The frozen tissue was then microtomed into sections (e.g., 20–50 μm) appropriate for autoradiography, with the slices being approximately perpendicular to the long TLD axis. The resulting micro-TLD chips were removed, cleaned, air dried, and read in the same reader and with the same heat cycle as is used for the mini-TLD.

The uniformity of response of the micro-TLD was investigated by Wessels and Griffith[31] and by Heidorn *et al.*[47] and by Langmuir *et al.*.[39] Mini-TLD were exposed to calibrated external beams under standard conditions. The dosimeters were then imbedded in suitable solid medium and microtomed as described above. Micro-TLD were selected at random from these samples and read. A standard deviation of 10% was observed in Ref. 31 while a standard deviation ranging from 22% to 32% was reported in the study Ref. 47, and a standard deviation of 29% (for 50-μm sections) and 50% for 30-μm sections was reported in Ref. 39. The reason for the very different dispersions measured by different investigators is not, at present, understood but may be related to differences in TLD grain size. Heidorn[47] using a dissection microscope at 50X magnification, observed differences in grain size distribution between micro-TLD batches. Some micro-TLD contained large $CaSO_4$:Dy crystals, some had large voids due to crystals pulled from

the Teflon matrix by the microtome knife and some had a uniform distribution of small crystals. In general, slice thickness must be carefully regulated to improve light output uniformity.

There is no predictive index to determine the uniformity of response of a group of micro-TLD. However precision can be optimized by individually calibrating each micro-TLD as described by Heidorn, *et al.*[47] Through use of individual calibration factors, standard deviations of 12% were achieved in measurement of a known external beam dose gradient.

IV. COMBINATION OF TECHNIQUES

When absorbed doses measured with micro-TLD extracted from autoradiographs were considered in the context of the optical density in the region from which the TLD had been removed, qualitative agreement was observed between high absorbed dose and high optical density for tumors[7,34] and spheroids.[39] Good agreement was found between micro-TLD measurements and calculated dose gradients in a spheroid model[39] where physical decay of I-131 provided the only time dependence. While such agreement is self evident in situations where physical decay provides the only time dependence, it is not assured in tumors with more complex pharmacokinetics. Additionally, the micro-TLD provide the magnitude of the absorbed dose. The combined use of ARG and thermoluminescent dosimetry demonstrated quantitatively that large absorbed dose gradients can be found in tumors treated with RIT. In one sample[7] a 200% dose variation was measured within a single slice and a 400% variation was observed between slices which were only 500 μm apart.

Since the micro-TLD integrate absorbed dose over time, no biokinetic model is needed to calculate the dose at the site of the TLD. Wessels *et al.*[48] have suggested that the micro-TLD be used to calibrate the optical density of the autoradiographs. That is, rather than associate optical density with specific activity, one could make a direct relationship between OD and absorbed dose via the micro-TLD. Ideally, there should be several micro-TLD at sites in a slice with different OD's allowing an individualized calibration curve (OD versus dose measured by the TLD) to be generated for a particular tissue sample. Since the TLD integrates over the spatial as well as the temporal activity distribution, there is also no need to use a point source function or to correlate the activity distribution in different slices. Instead, the OD would be translated directly to absorbed dose through the calibration curve. The accuracy of this technique (which estimates the absorbed dose via interpolation between micro-TLD readings at two or three points per slice) versus the pharmacokinetic modeling approach discussed previously requires further investigation. The use of electronic probes such as MOSFET detectors[49] may be helpful in providing *in vivo* measurements of dose versus time at a few locations in tissue.

Theoretically, both approaches have potential drawbacks and possible advantages. Autoradiography, by definition, is a destructive process in relation to unique tumor architecture. Modeling approaches used to correct autoradiographic information for time varying concentrations are constrained to use average bulk tumor biodistribution data or repetitive activity distribution phenomena (e.g., time-varying but predictable tumor rim enhancement) to correct for antibody pharmacokinetics and gross tumor heterogeneity. The combination TLD/ARG methods do include a directly measured time integration factor in the absorbed dose along with a dose distribution which is based on ARG. However, some uncertainty is entered into this method by assuming that the "local" assignment of an absorbed dose value to a particular optical density value applies universally throughout the tumor. Perhaps a safe starting point or working hypothesis for both methods is that any correction for time dependence of antibody pharmacokinetics is superior to simply using physical decay to derive a cumulated activity distribution from autoradiography patterns.

V. DISCUSSION

The goal of the dosimetric studies presented above is to help relate the therapy technique of RIT to the outcome (e.g., tumor regression). ARG demonstrates that tumors often exhibit activity distributions which are inhomogeneous on a distance scale of $10-10^4$ μm. Both calculations and *in vivo* TLD measurements show that these spatial activity variations are associated with large dosimetric variations on the same distance scales. The validity of approximating the tumor dose distribution by a single average absorbed dose may therefore be questioned.

In addition to spatial dosimetric inhomogeneities, other factors may alter the biological effectiveness of the absorbed dose. Among these are the variation of the dose rate with time and the possible relationship of cell viability to local activity deposition. An understanding of the interrelationships between tumor pharmacokinetics and spatial and temporal variations of dose rate and total dose deposition may be required for reliable prediction of the outcome of tumor therapy. However, a necessary step toward this goal is improved quantitation of absorbed dose at the multicellular level in tumors.

ACKNOWLEDGMENTS

This work was supported in part by NCI Grants No. CA33572, CA43904 and CA44173.

[1]A. W. Rogers, *Techniques of Autoradiography* (Elsevier/North-Holland Biomedical, New York, 1979).

[2]W. K. Sinclair, J. D. Abbatt, H. E. A. Farran, E. B. Harriss, and L. F. Lamerton, "A quantitative autoradiographic study of radioiodine distribution and dosage in human thyroid glands," Br. J. Radiol. **29**, 36–41 (1950).

[3]T. K. Lewellen, M. M. Graham, and A. M. Spence, "Quantitative autoradiography using a personal computer," J. Nucl. Med **27**, 549–554 (1986).
[4]Y. Yonekura, A. B. Brill, P. Som, G. W. Bennett, and I. Fand, "Quantitative autoradiography with radiopharmaceuticals, part 1: Digital film analysis system by videodensitometry: Concise Communication," J. Nucl. Med. **24**, 231–237 (1983).
[5]P. L. Jones, B. M. Gallagher, and H. Sands, "Autoradiographic analysis of monoclonal antibody distribution in human colon and breast tumor xenografts," Cancer Immunol. Immunother. **22**, 134–143 (1986).
[6]J. M. Esteban, J. Schlom, F. Mornex, and D. Colcher, "Radioimmunotherapy of athymic mice bearing human colon carcinomas with monoclonal antibody B72.3: Histologic and autoradiographic study of effects on tumors and normal organs," Eur. J. Cancer Clin. Oncol. **23**, 643–655 (1987).
[7]M. H. Griffith, E. D. Yorke, B. W. Wessels, G. L. DeNardo, and W. P. Neacy, "Direct dose confirmation of quantitative autoradiography with micro-TLD measurements for radioimmunotherapy," J. Nucl. Med. **29**, 1795–1809 (1988).
[8]J. L. Humm, "Dosimetric aspects of radiolabeled antibodies for tumor therapy," J. Nucl. Med. **27**, 1490–1497 (1986).
[9]C. S. Kwok, W. V. Prestwich, and B. C. Wilson, "Calculation of radiation doses for non uniformly distributed beta and gamma radionuclides in soft tissues," Med. Phys. **12**, 405–412 (1985).
[10]V. K. Langmuir and R. M. Sutherland, "Dosimetry models for radioimmunotherapy," Med. Phys. **15**, 867–873 (1988).
[11]R. W. Howell, D. V. Rao, and K. Sastry, "Macrodosimetry for radioimmunotherapy:Nonuniform activity distributions in solid tumors," Med. Phys. **16**, 66–74 (1989).
[12]*Applied Thermoluminescence Dosimetry*, edited by M. Oberhofer and A. Scharmann (Adam Hilger Ltd, Bristol, 1981).
[13]*Thermoluminescence and Thermoluminescent Dosimetry, Vols. I, II, and III*, edited by Y. L. Horowitz (CRC, Inc., Boca Raton, FL, 1984).
[14]J. L. Humm, L. M. Chin, R. C. Lanza, C. M. Schaefer, M. Speidel, and R. L. Greene, "Digital imaging for autoradiography," in *Computed Digital Radiography in Clinical Practice* edited by R. E. Greene and J. W. Oestmann (Thieme Medical Publishers, Inc., New York, 1992), pp. 167–172.
[15]R. Mayer, L. E. Dillehay, Y. Zhang, Y. Shao, S. Song, W. C. Lam, and J. R. Williams, "New method for microdosimetry in radioimmunotherapy using GAF TM chromic media," Antib. Immunoconj. Radiopharm. **5**, 336 (1992).
[16]R. L. Vessella, P. H. Lange, D. F. Palme, R. K. Chiou, M. K. Elson, and B. W. Wessels, "Radioiodinated monoclonal antibodies in the imaging and treatment of human renal cell carcinoma xenografts in nude mice," in *Antibody Mediated Delivery Systems*, edited by J. D. Rodwell (Marcel Dekker, Inc., NY, 1988), pp. 245–282.
[17]P. L. Roberson, D. J. Buchsbaum, D. B. Heidorn, and R. K. Ten Haken, "Three-dimensional tumor dosimetry for I-131 labeled MoAb using serial autoradiography," Int. J. Radiat. Oncol. Biol. Phys. **24**, 329–334 (1992).
[18]L. J. Van Battron and H. Huizenga, "Film dosimetry of clinical electron beams," Int. J. Radiat. Oncol. Biol. Phys. **18**, 69–76 (1990).
[19]K. E. Eklund and J. R. Williams, "A method for quantitative autoradiography over stained sections of tumors exposed *in vivo* to radiolabeled antibodies," Int. J. Radiat. Oncol. Biol. Phys. **21**, 1635–1642 (1992).
[20]R. Loevinger, E. M. Japha, and G. L. Brownell, "Discrete radioisotope sources," in *Radiation Dosimetry*, edited by G. J. Hine and G. L. M. Brownell (Academic,, NY, 1956), pp. 693–799.
[21]W. V. Prestwich, J. Nunes, and C. S. Kwok, "Beta dose point kernels for radionuclides of potential use in radioimmunotherapy," J. Nucl. Med. **30**, 1036–1046 (1989).
[22]P. K. Leichner, W. G. Hawkins, and N. C. Yang, "A generalized empirical point source function for beta particle dosimetry," Antib. Immunoconj. Radiopharm. **2**, 125–144 (1989).
[23]P. K. Leichner and C. S. Kwok, "Tumor dosimetry in radioimmunotherapy:Methods of calculation for beta particles," Med. Phys. **20**, 529–534 (1993).
[24]P. L. Roberson, D. J. Buchsbaum, D. B. Heidorn, and R. K. Ten Haken, "Variations in 3-D distributions of tumor uptake and dose deposition for I-131 labeled MoAb," Antib., Immunoconj. Radiopharm. **4**, 43 (1991).
[25]R. McFadden and C. S. Kwok, "Mathematical model of simultaneous diffusion and binding of antitumor antibodies in multicellular human tumor spheroids," Cancer Res. **48**, 4032–4037 (1988).
[26]K. Fujimori, D. G. Covell, J. E. Fletcher, and J. N. Weinstein, "A modeling analysis of monoclonal antibody percolation through tumors: A binding site barrier," J. Nucl. Med. **31**, 1191–1198 (1990).
[27]P. K. Leichner, N. C. Yang, B. W. Wessels, W. G. Hawkins, S. E. Order, and J. L. Klein, "Dosimetry and treatment planning in radioimmunotherapy," in *The Present and Future Role of Monoclonal Antibodies in the Management of Cancer*, edited by J. M. Vaeth and J. L. Meyer (Karger, Basel, Switzerland, 1990), pp. 109–120.
[28]D. G. Covell, J. Barbet, O. D. Holton, C. D. Black, R. J. Parker, and J. N. Weinstein, "Pharmacokinetics of monoclonal immunoglobulin Gl, F $(ab')_2$ and Fab' in mice," Cancer Res. **46**, 3969–3978 (1986).
[29]J. A. Carrasquillo, P. Sugarbaker, D. Colcher, J. C. Reynolds, J. Esteban, G. Bryant, A. M. Keenan, P. Perentesis, K. Yokoyama, D. E. Simpson, P. Ferroni, R. Farkas, J. Schlom, and S. M. Larson, "Radioimmunoscintigraphy of colon cancer with I-131 labeled B72.3 monoclonal antibody," J. Nucl. Med. **29**, 1022–1030 (1988).
[30]F. Buchegger, A. Vacca, S. Carrel, M. Schreyer, and J-P. Mach, "Radioimmunotherapy of human colon carcinoma by I-131 labeled monoclonal anti CEA antibodies in a nude mouse model," Int. J. Cancer **41**, 127–134 (1988).
[31]B. W. Wessels and M. H. Griffith, "Miniature thermoluminescent dosimeter absorbed dose measurements in tumor phantom models," J. Nucl. Med. **27**, 1308–1314 (1986).
[32]B. W. Wessels, R. L. Vessella, D. F. Palme, J. M. Berkopec, G. K. Smith, and E. W. Bradley, "Radiobiological comparison of external beam irradiation and radioimmunotherapy in renal cell carcinoma xenografts," Int. J. Radiat. Oncol. Biol. Phys. **17**, 1257–1263 (1989).
[33]J. L. Klein, T. H. Nguyen, P. Laroque, K. A. Kopher, J. R. Williams, B. W. Wessels, L. E. Dillehay, J. Frincke, S. E. Order, and P. K. Leichner, "Yttrium-90 and I-131 radioimmunoglobulin therapy of an experimental human hepatoma," Cancer Res. **49**, 6383–6389 (1989).
[34]J. A. Williams, B. W. Wessels, J. A. Edwards, K. A. Kopher, P. M. Wanek, M. D. Wharam, S. E. Order, and J. L. Klein, "Targeting and therapy of human glioma xenografts *in vivo* utilizing radiolabeled antibodies," Cancer Res. (Suppl.) **50**, 974s–979s (1990).
[35]D. F. Palme, J. M. Berkopec, B. W. Wessels, M. K. Elson, P. H. Lange, and R. L. Vessella, "Dosimetry and pharmacokinetics of monoclonal antibody A6H with human renal cell carcinoma xenografts: Single dose study," Int. J. Nucl. Med. Biol. **18**, 527–537 (1991).
[36]R. Wessely, H. Bihl, E. Friedrich, and S. Matzku, "Assessment of radiation dose distribution in xenografts," in *Monoclonal Antibodies: Application in Clinical Oncology*, edited by A. Epenetos (Chapman and Hall Medical, NY, 1991), pp. 315–322.
[37]R. K. Chiou, B. W. Wessels, M. Woodson, and C. Limas, "Study of clinical thermoluminescent dosimeters (CL.TLD) in direct measurement of absorbed radiation dose for radioimmunotherapy," Radiat. Appl. Isot. **42**, 181–186 (1991).
[38]J. Y. C. Wong, L. E. Williams, A. J. Demidecki, B. W. Wessels, and X. W. Yan, "Radiobiologic studies comparing yttrium-90 irradiation and external beam irradiation *in vitro*," Int. J. Radiat. Oncol. Biol. Phys. **20**, 715–722 (1991).
[39]V. K. Langmuir, B. W. Wessels, H. L. Mendonca, E. D. Yorke, and L. Montilla, "Comparisons of sectioned micro-tld dose measurements with predicted dose from I-131 labeled antibody," Med. Phys. **19**, 1213–1218 (1992).
[40]A. J. Demidecki, L. E. Williams, and J. Y. C. Wong, "Calibration of thermoluminescent dosimeters for beta radiation," Antib. Immunoconj. Radiopharm. **4**, 52 (1991).
[41]A. J. Demidecki, L. E. Williams, J. Y. C. Wong, B. W. Wessels, E. D. Yorke, M. Strandh, and S. Strand, "Considerations on the calibration of small thermoluminescent dosimeters (TLDs) used for measurement of beta particle absorbed doses in liquid environments," in press, Med. Phys. (1993).
[42]D. B. Heidorn, personal communication.
[43]J. S. W. Stewart, V. Hird, D. Snook, M. Sullivan, G. Hooker, N. Courtenay-Luck, G. Sivdapenko, M. Griffiths, M. J. Meyers, H. E. Lambert, A. J. Munro, and A. A. Epenetos, "Intraperitoneal radioimmunotherapy for ovarian cancer: Pharmacokinetics, toxicity and efficacy of I-131 labeled monoclonal antibodies," Int. J. Radiat. Oncol. Biol. Phys. **16**, 405–413 (1989).
[44]A. S. Pradhar and R. C. Bhatt, "Graphite mixed $CaSo_4$:Dy teflon TLD discs for beta dosimetry," Phys. Med. Biol. **22**, 873–879 (1977).
[45]A. Svenberg, personal communication.

[46]S-E Strand, A. Svenberg, M. Strandh, and K. Norrgren, "Parameters affecting the accuracy of *in vivo* dosimetry with mini-TLD," Med. Phys. **19**, 781 (1992).
[47]D. B. Heidorn, D. J. Buchsbaum, P. L. Roberson, and R. K. Ten Haken, "A sensitivity study of micro-TLD's for *in vivo* dosimetry of radiolabeled antibodies," Med. Phys. **18**, 1195–1199 (1991).
[48]B. W. Wessels and E. D. Yorke, *Biology of Radionuclide Therapy*, edited by G. L. DeNardo, J. P. Lewis, A. Raventos, and R. W. Burt (ACNP Publication No. 308, Washington, DC, 1989), pp. 216–222.
[49]D. J. Gladstone and L. M. Chin, "Automated data collection and analysis system for MOSFET radiation detectors," Med. Phys. **18**, 542–548 (1991).